Instrumentation Developments for Heat Transfer Measurement under Rotating Conditions

R. W. Ainsworth, J. L. Allen, M. A. Hilditch
and M. L. G. Oldfield

University of Oxford
Department of Engineering Science

Transient wind tunnels, firstly in the form of shock tunnels and more recently in the form of isentropic light piston tunnels and blowdown tunnels, have long been found to be convenient vehicles for heat transfer measurements. One reason for this is the ease with which thin film thermometry acting on a semi-infinite substrate may be applied to infer heat transfer rate for short timescales. A review of these techniques may be found in Schultz and Jones[1], and Oldfield and Ainsworth[2] in the present proceedings.

More recently there has been considerable interest in making heat transfer measurements in the rotating frame, trying to simulate the environment of the h.p. turbine stage. Internationally, there are currently three facilities aimed at researching the area of rotating heat transfer measurement, at MIT and Calspan in the USA, and in Oxford. Each uses a different form of wind tunnel and each uses a variation on a theme as far as instrumentation is concerned.

At MIT, Epstein[3] makes use of a blowdown type facility with run times of order 1 second, and utilising a calorimeter type gauge to infer heat transfer rate. Dunn's work[4] at Calspan uses a shock tunnel with run time of order 10 msec +, instrumented with discrete pyrex semi-infinite thin film thermometer gauges let into the surface. Finally, the work of Ainsworth et al.[5,6] has extended the Isentropic Light Piston Tunnel into a fully 3-D rotating capability with run time of order .1 sec., developing the layered gauge technology first suggested by Doorly and Oldfield[7], into a practical system for heat flux measurement on a 3-D surface subjected to high gravitational accelerations due to rotation.

This new "layered" technology has been at the heart of the Oxford developments. The standard thin film thermometers previously used in Oxford on semi-infinite substrates (Fig. 1) were applied by a process of painting on liquid platinum (Engelhard 05-X) directly onto the substrate material and firing at high temperature. Now, by suitable choice of vitreous enamel, an insulating (thermally and electrically) layer could be applied to a metal substrate, again allowing the application of thin film sensors, but this time to a 3-D profile, the whole capable of withstanding the necessary (32,000 g) high centrifugal accelerations.

The mathematics describing the more complex heat flux measurement were developed by Doorly[8], and one key equation relating heat flux history to surface temperature history is given in Fig. 2. Basically, at high frequencies the enamel layer appears as if it were an infinitely thick substrate, whilst at low frequencies, the properties of the underlying metal substrate dominate. The response of the layered gauge as a function of frequency for different enamel thicknesses is given in Fig. 3.

In the Oxford rotor project, these developments lead to the successful production of heat flux instrumentation on a 3-D blade profile (Fig. 6) capable of withstanding the arduous conditions imposed in the rotating turbine. A paramount requirement was to ensure that the signal levels produced by the gauges when subjected to heat flux were protected to the maximum extent from any noise degradation associated with rotation. From an early date it was decided to amplify the heat flux voltage signals within the rotating frame prior to transmission through the slip-ring, to minimise any slip-ring noise introduced. Since the sensitivity of the output of the gauge (voltage fluctuation, proportional to surface temperature fluctuation) for a given input (heat flux) fell off as the square root of increasing frequency, an in-shaft amplification system was specified with the inverse characteristic, i.e. one where the gain increased in a manner proportional to the square root of increasing frequency. In practice, this was to be achieved by a low noise fast response amplifier[5], configured in the non-inverting mode with a variable impedance in the feedback leg giving a series of breakpoints in the gain-frequency characteristic. The inverse of the gauge sensitivity and the amplifier characteristic are overplotted in Fig. 6, whilst a comparison of the measured electrical response compared with its predicted companion is given in Fig. 7.

Finally, the overall system gain (product of gauge sensitivity and amplifier gain) as a function of frequency is given in Fig. 8. The overall variation in gain level is kept to a low value, optimising the performance of the data acquisition system's A/D convertors.

The design of the in-shaft electronics, serving 8 thin film gauges simultaneously formed a major part of the research effort. The hardware had to withstand rotation at speeds up to 10,000 rpm with no change in performance, and was designed to permit the servicing of up to 128 thin film heat transfer gauges without the need for altering wiring configurations. This was achieved by the use of two multiplexers, multiplexing the instant current source to the thin film gauge, and the relevant gauge voltage output to the operational amplifier. A portion (approximately one quarter) of the double sided pcb in-shaft electronics may be seen in Figs. 9a and 9b.

A schematic of the overall data acquisition system is shown in Fig. 10, where it will be seen that a differential buffer amplifier and filter was used to condition the signals emerging from the slip ring. This unit, Fig. 11, was designed around the AMP-05 fast response J-FET differential input instrumentation amplifier, provided a high performance unit which would be placed close to the slip-ring, enabling transmission to the data acquisition system at a high level.

A considerable effort was expended within this project in developing a calibration system which would enable the enamel thickness to conductivity parameter to be evaluated for any gauge. Following the schematic of Fig. 12, the surface temperature rise of a semi-infinite insulator alone, or metal alone, follows a straight line when plotted against the square root of time. For the enamelled gauge, the behaviour in short time follows that of insulator and in long time that of metal with a 'switch' area in the middle. Determination of the 'switch' point in time can be shown (Doorly[7]) to give the relevant thickness/conductivity parameter. An experiment was devised using an Argon-Ion laser (Fig. 13), to pulse the gauge with radiant heat and measure the resulting response of the gauge. A typical result from this experiment is given in Fig. 14, together with the reconstructed input heat flux in Fig. 15. Digital signal processing techniques are used throughout the project to turn voltage output signals back into applied heat flux or surface temperature histories (Doorly[8]).

The end part of these developments is their application to a rotating heat transfer experiment, Ainsworth et al.[5,6]. Essentially results in two time-scales are of interest. Blade-vane interactions are occurring at a frequency of approximately 6 kHz, so unsteady heat transfer measurements are made with a bandwidth of 80 - 100 kHz (Fig. 16). Equally, the mean heat transfer rates experienced around the rotor profile during rotation at engine conditions are of interest, and a typical plot of mean heat flux against time is shown in Fig. 17.

In summary, much development work has been required to allow the measurement of unsteady and mean heat flux to a turbine stage under engine representative condition, involving producing instrumentation which can be applied to a three-dimensional profile which will endure the centrifugal forces, developing in-shaft electronics for signal conditioning in the rotating frame, developing the necessary calibration procedures, and devising digital signal processing routines for analysing the data. These developments are now complete and, although no doubt further refinements will always be made, the first measurements from the new rotor facility have been obtained.

References

1. Schultz, D. L. and Jones, T. V., Heat Transfer Measurements in a Short Duration Hypersonic Facility, AGARD Paper No. 165, 1973.

2. Oldfield, M. L. G. and Ainsworth, R. W., The Use of Wide-Bandwidth Heat Transfer Gauges to Diagnose Unsteady Turbomachinery Flows, Present Proceedings.

3. Epstein, A. H., Guenette, G. R., Norton, R. J. G. and Yuzhan, C., High Frequency Response Heat Flux Gauge for Metal Blading, AGARD Paper No. 30, 1985.

4. Dunn, M. G., Heat Flux Measurements for the Rotor of a Full-Stage Turbine, Part I - Time Averaged Results, ASME J. Turbomachinery, Vol. 108, No. 1, 1986.

5. Ainsworth, R. W., Schultz, D. L., Davies, M. R. D., Forth, C. J. P., Hilditch, M. A., Oldfield, M. L. G. and Sheard, A. G., A Transient Flow Facility for the Study of the Thermofluid-dynamics of a Full Stage Turbine under Engine Representative Conditions, 33rd ASME Int. Gas Turbine Conference, Amsterdam, Paper No. 88-GT-144, 1988.

6. Ainsworth, R. W., Allen, J. L., Davies, M. R. D., Doorly, J. E., Forth, C. J. P., Hilditch, M. A., Oldfield, M. L. G., Sheard, A. G., Developments in Instrumentation and Processing for Transient Heat Transfer Measurement in Full Stage Model Turbine, 33rd ASME Int. Gas Turbine Conference, Amsterdam, Paper No. 88-GT-11, 1988.

7. Doorly, J. E. and Oldfield, M. L. G., The Theory of Advanced Heat Transfer Gauges, Int. J. Heat and Mass Transfer, Vol. 30, No. 6, pp. 1159 - 1168, 1987.

8. Doorly, J. E., Procedures for Determining Surface Heat Flux using Thin-Film Gauges on a Coated Metal Model in a Transient Test Facility, 32nd ASME Int. Gas Turbine Conference, Amsterdam, Paper No. 87-GT-95, 1987.

CONSTRUCTION OF THIN FILM GAUGE AS PREVIOUSLY USED IN OXFORD

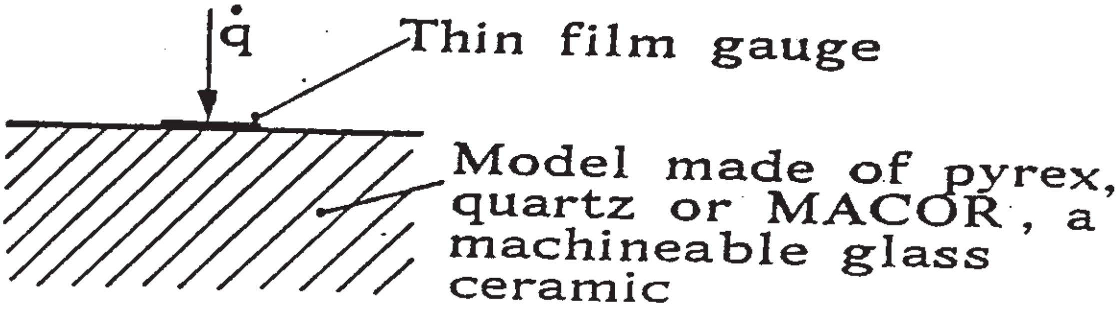

CONSTRUCTION OF THIN FILM GAUGE AS USED IN OXFORD ROTOR PROJECT

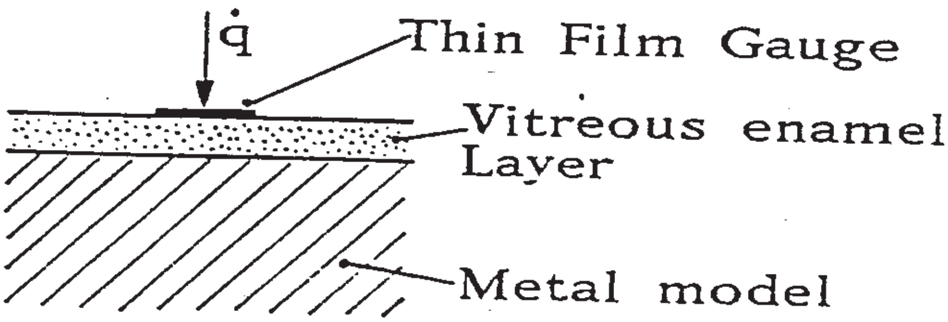

Fig. 1 Comparison between semi-infinite and layered approaches to thin film thermometry.

With Semi-infinite Metal Layer.

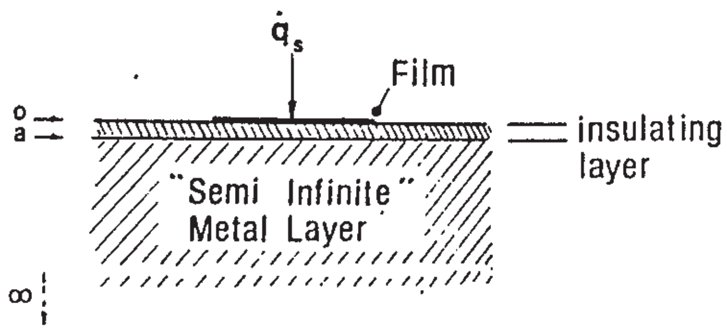

The governing equations are

$$\frac{\partial^2 T_1}{\partial x^2} = \frac{1}{\alpha_1}\frac{\partial T_1}{\partial t} \qquad 0 < x < a$$

$$\frac{\partial^2 T_2}{\partial x^2} = \frac{1}{\alpha_2}\frac{\partial T_2}{\partial t} \qquad a < x < \infty$$

Boundary conditions

$$-\dot{q} = k_1 \frac{\partial T_1}{\partial x} \qquad x=0$$

$$T_1 = T_2 \qquad x=a$$

$$k_1 \frac{\partial T_1}{\partial x} = k_2 \frac{\partial T_2}{\partial x} \qquad x=a$$

$$T_2 = 0 \qquad x=\infty$$

$$\dot{q}_s(s) = (\rho_1 c_1 k_1 s)^{1/2} \frac{\{1 - Ae^{(-2a\sqrt{s/\alpha_1})}\}}{\{1 + Ae^{(-2a\sqrt{s/\alpha_1})}\}} \bar{T}_s$$

$$A = \frac{\sqrt{\rho_1 c_1 k_1} - \sqrt{\rho_2 c_2 k_2}}{\sqrt{\rho_1 c_1 k_1} + \sqrt{\rho_2 c_2 k_2}}$$

T = surface temperature

k = thermal conductivity

α = thermal diffusivity $(\frac{k}{\rho c})$

ρ = density

c = specific heat capacity

1 - enamel layer

2 - metal layer

Fig. 2 Governing equations for layered gauges.

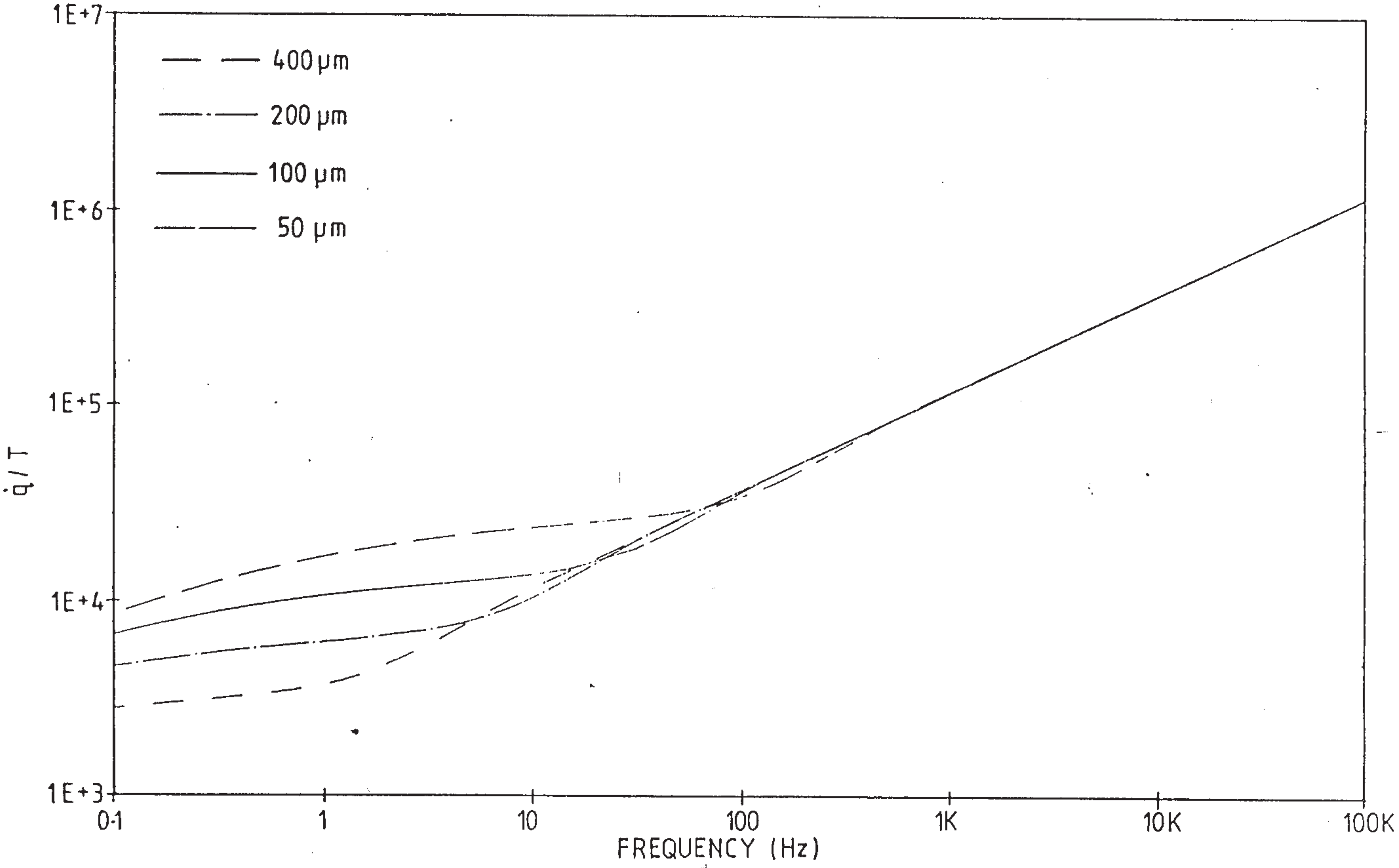

Fig. 3 Frequency response of layered gauges of various enamel thicknesses

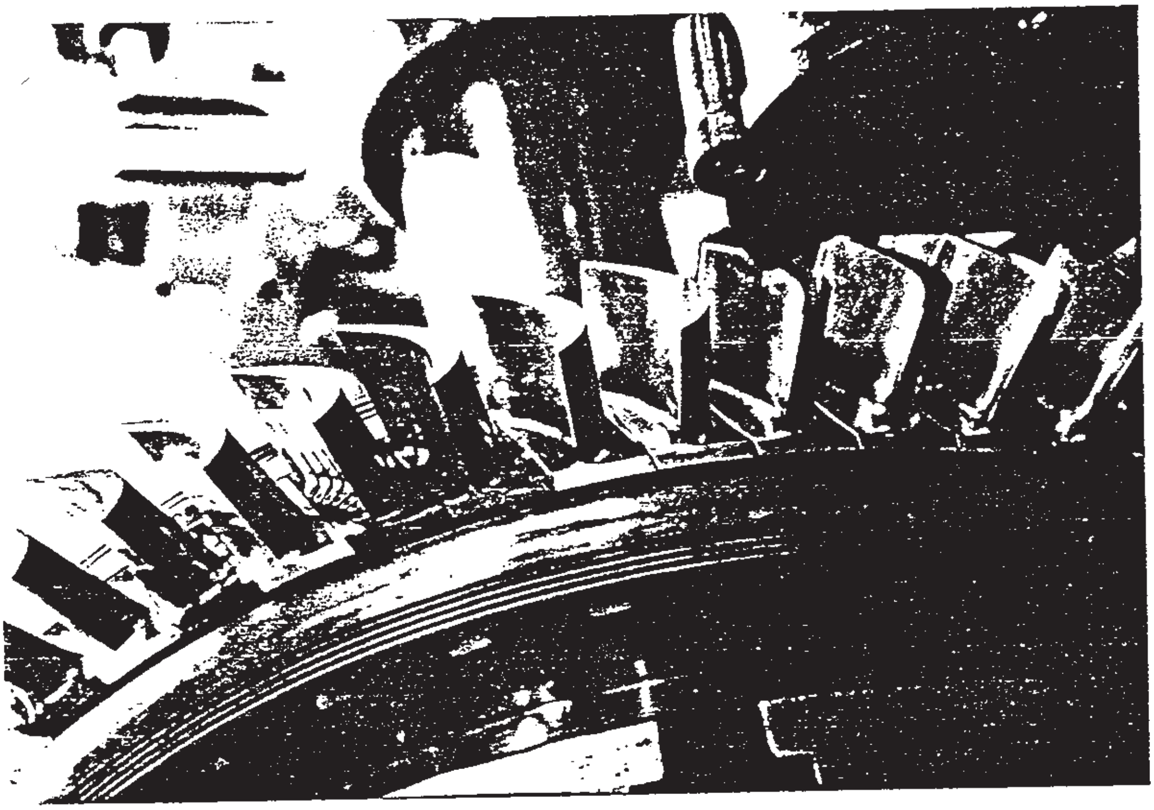

Fig. 4 Enamelled and instrumented heat flux blades mounted on rotor disc.

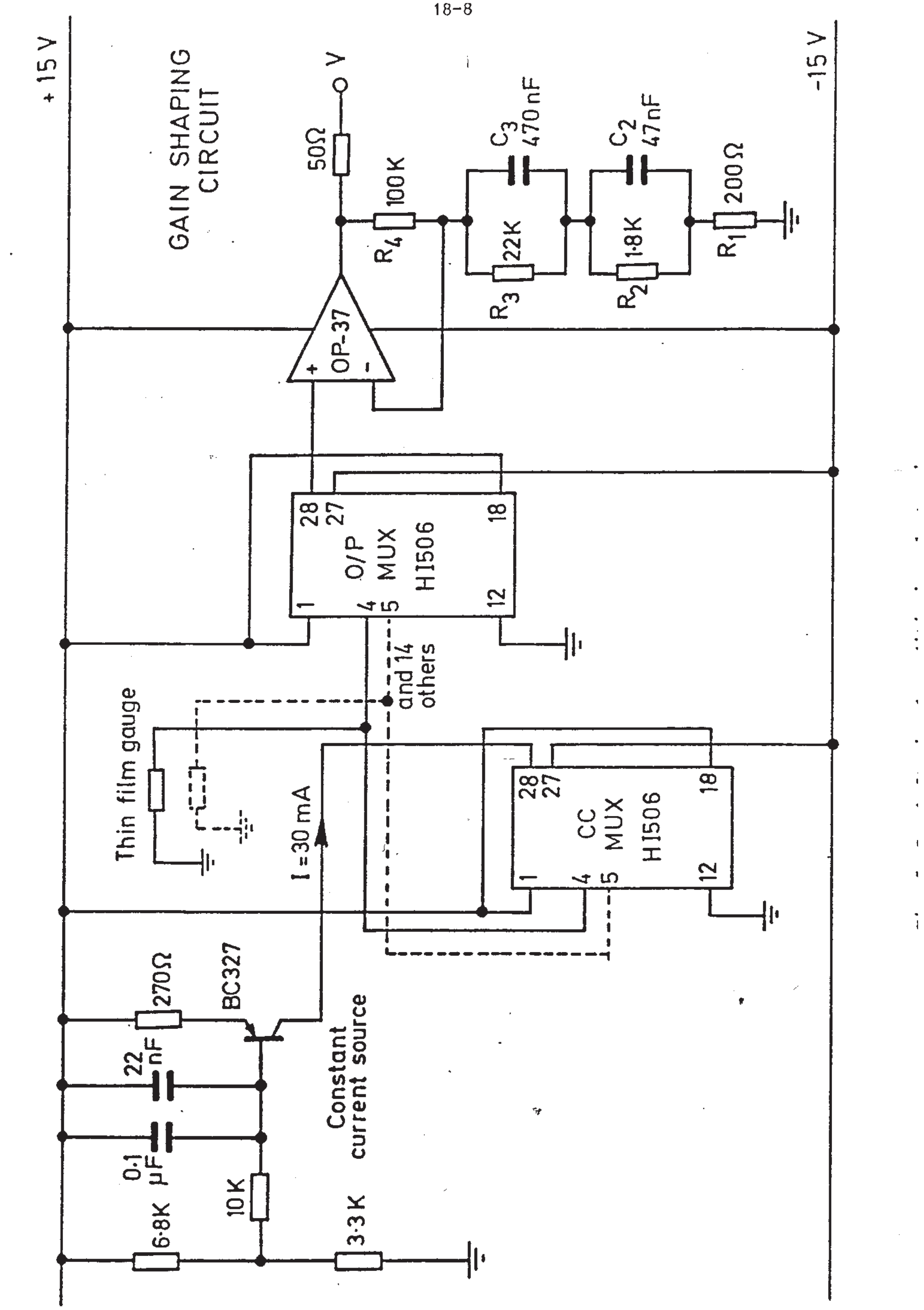
GAIN SHAPING CIRCUIT
+15 V
-15 V
V
50Ω
100K
R_4
OP-37
+
-
C_3
470 nF
22K
R_3
C_2
47nF
1·8K
R_2
200Ω
R_1
O/P
MUX
HI506
28
27
18
1
4
5
12
and 14 others
Thin film gauge
I = 30 mA
CC
MUX
HI506
28
27
18
1
4
5
12
270Ω
BC327
22 nF
0·1 μF
10K
6·8K
3·3K
Constant current source

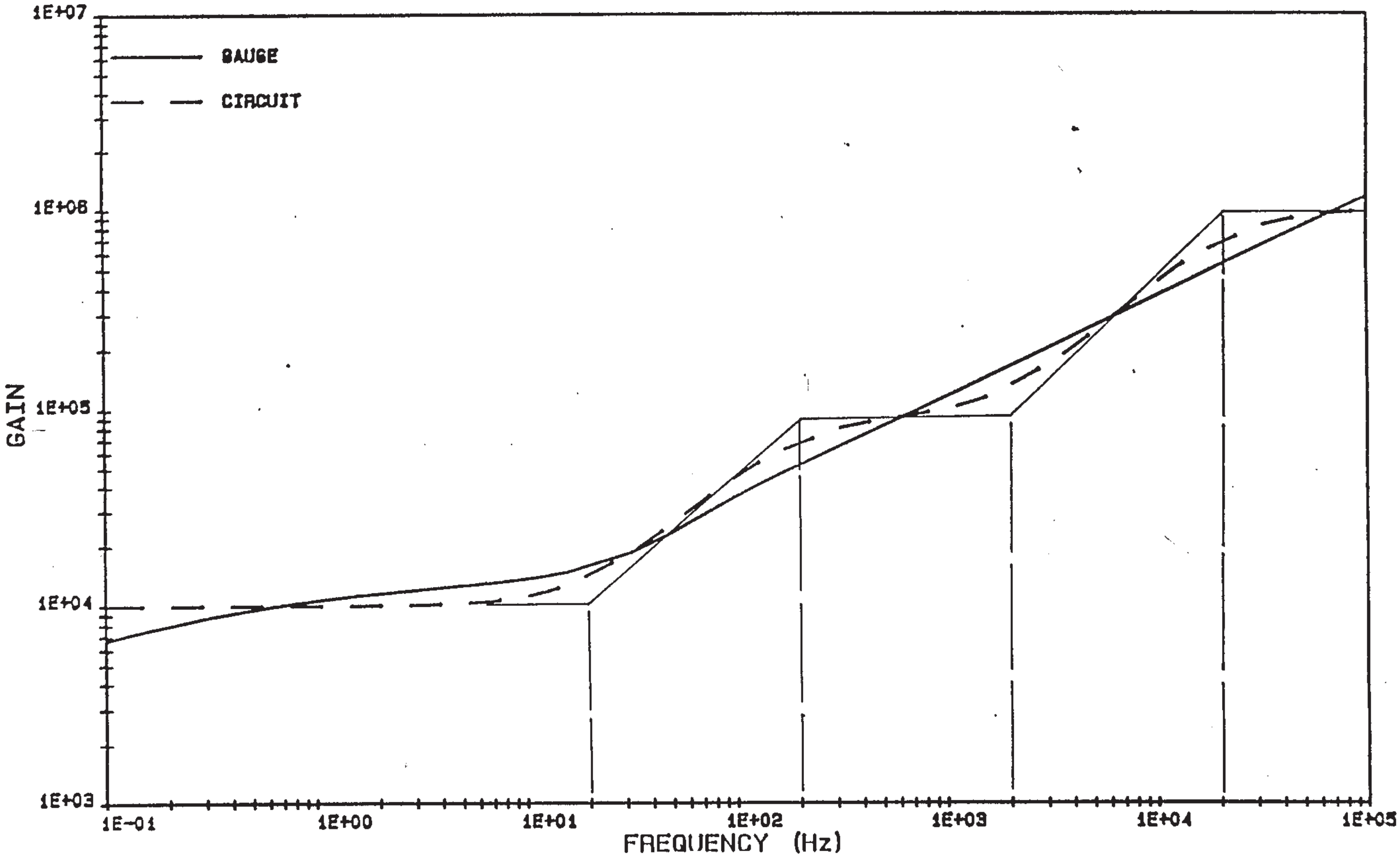
GAUGE
CIRCUIT
GAIN
1E+07
1E+06
1E+05
1E+04
1E+03
1E-01
1E+00
1E+01
1E+02
1E+03
1E+04
1E+05
FREQUENCY (Hz)

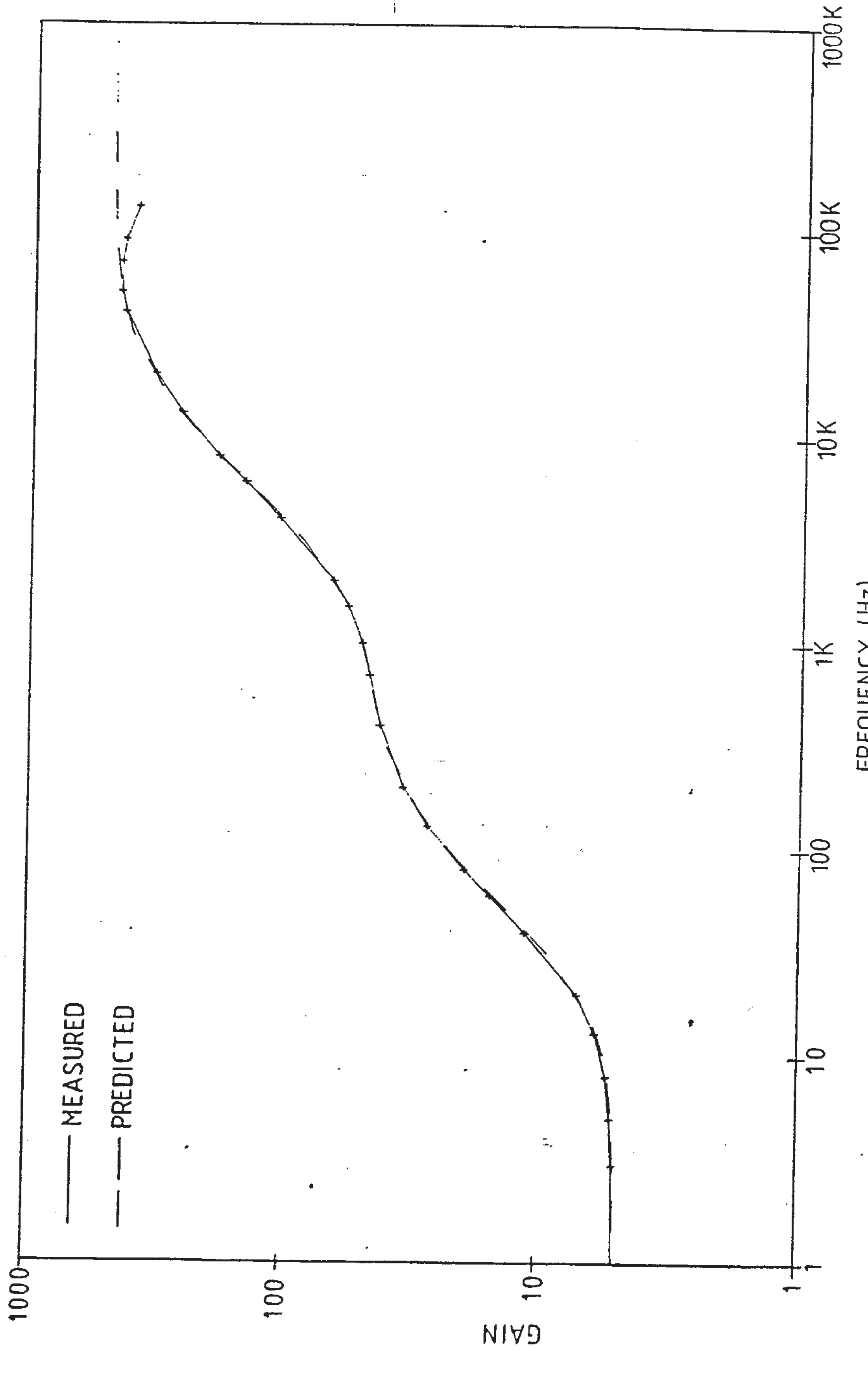

MEASURED
PREDICTED
GAIN
1000
100
10
1
FREQUENCY (Hz)
1
10
100
1K
10K
100K
1000K

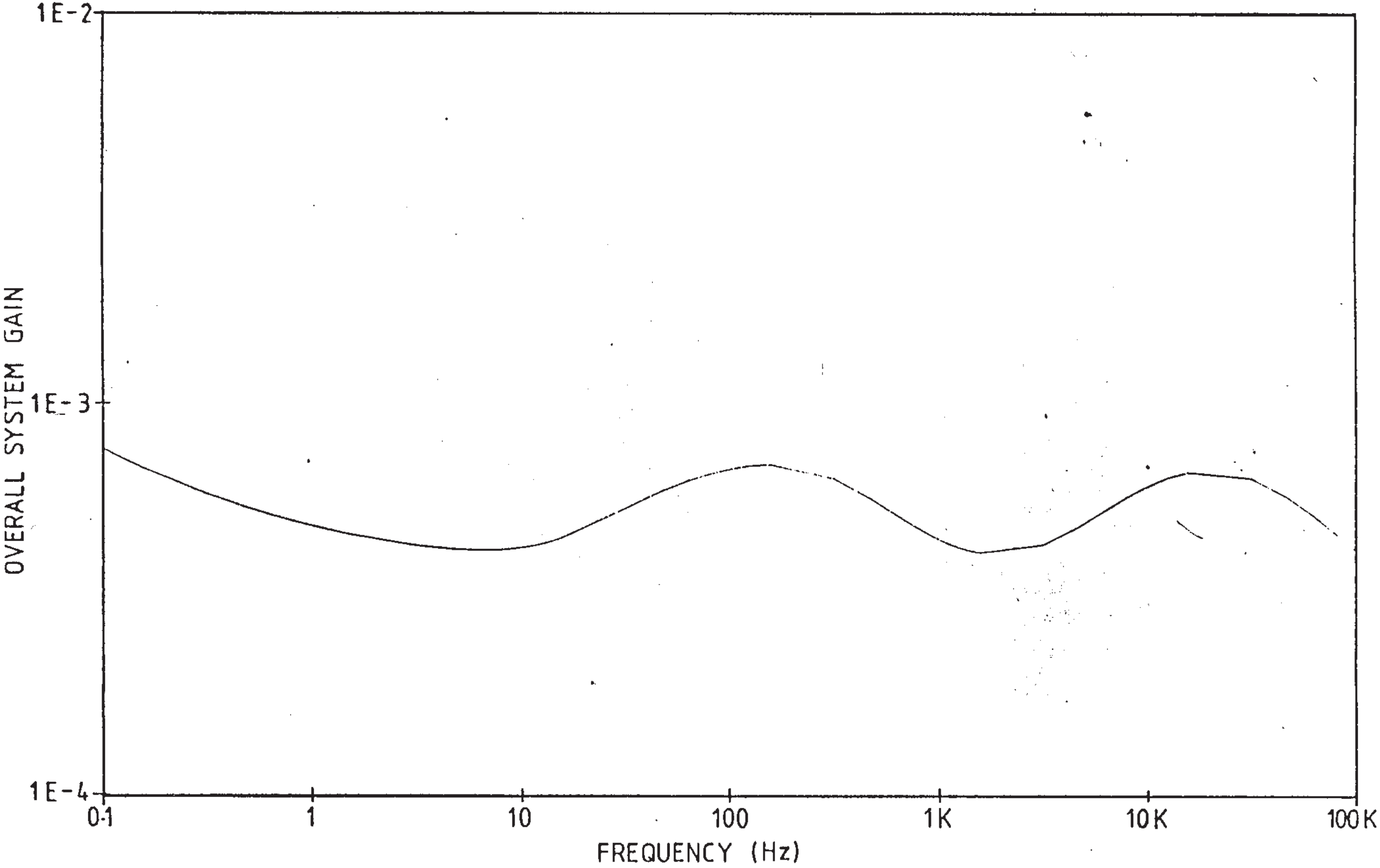

Fig. 8 Product of gauge sensitivity with conditioning gain as a function of frequency.

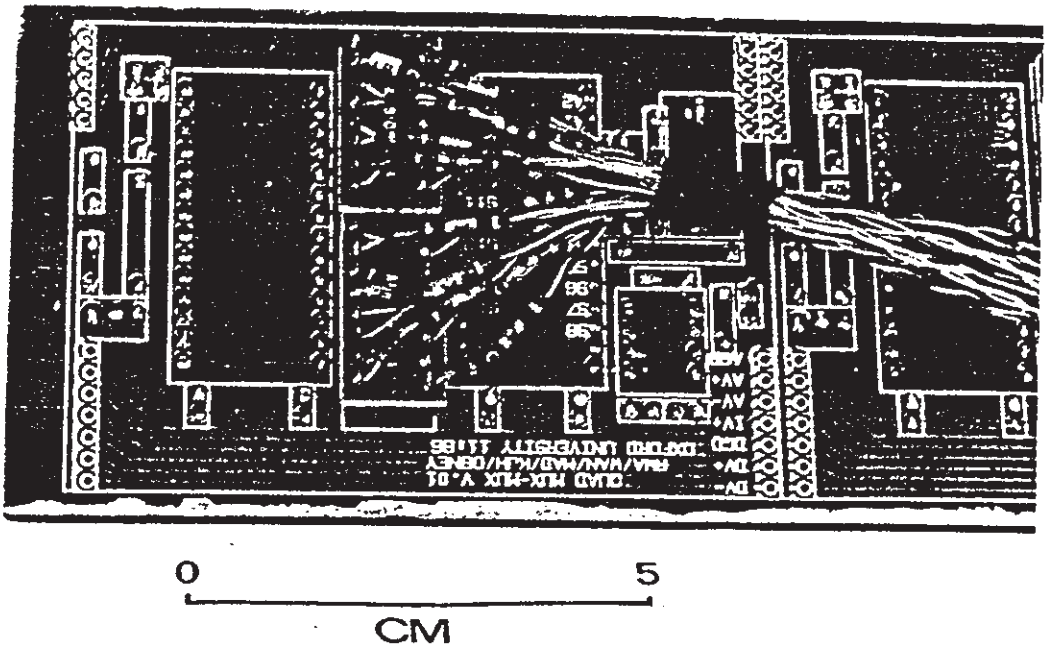

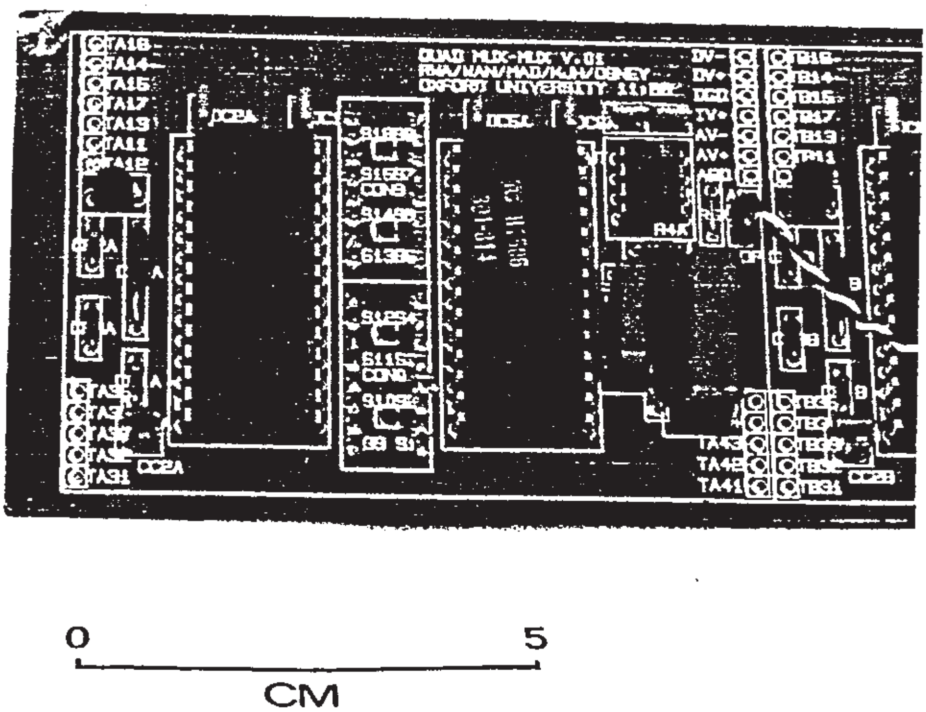

Fig. 9 Photograph of one quarter (both sides) of the in-shaft electronics.

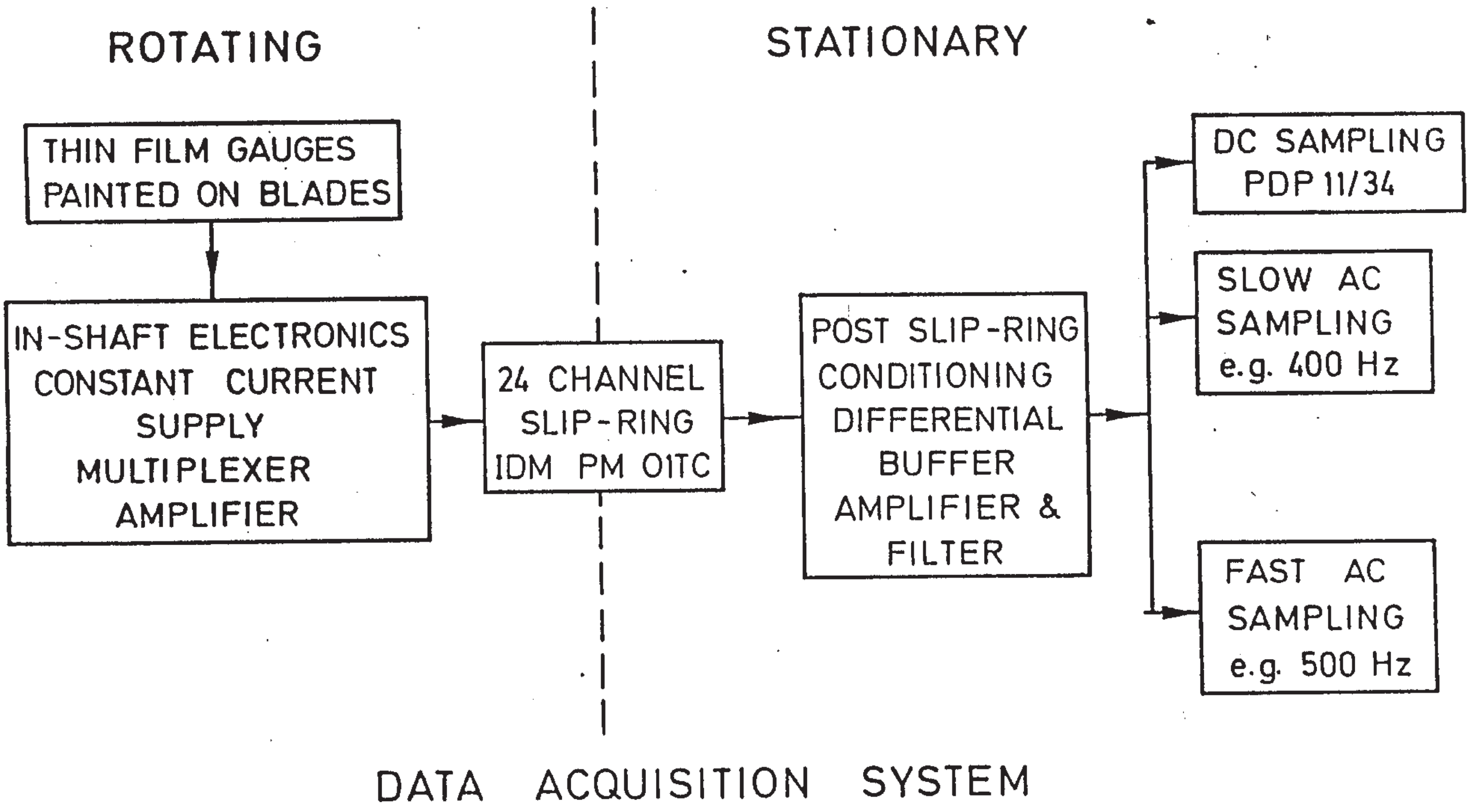

Fig. 10 Data acquisition system.

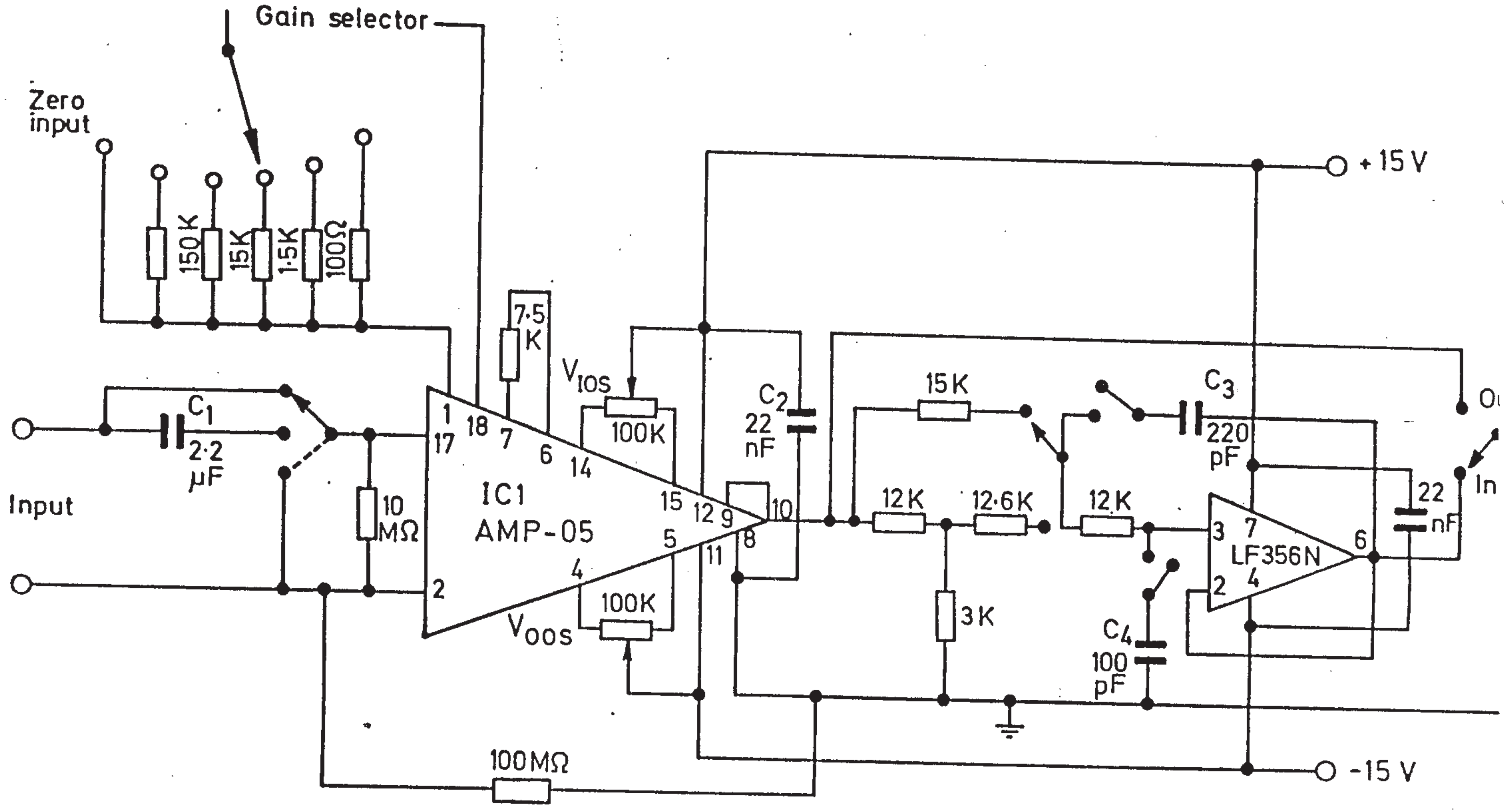

DIFFERENTIAL AMPLIFIER

÷5 ATTENUATOR

LP FILTER

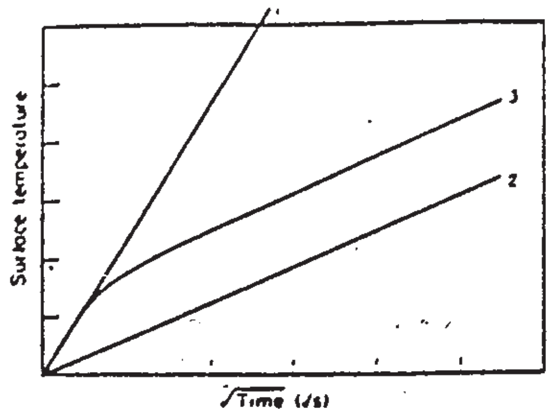

Fig.. 12 Predicted Surface Temperature Rise For Step in Heat Transfer at the Surface of : (1) Insulator Alone, (2) Metal Alone, (3) Insulator Coated Metal.

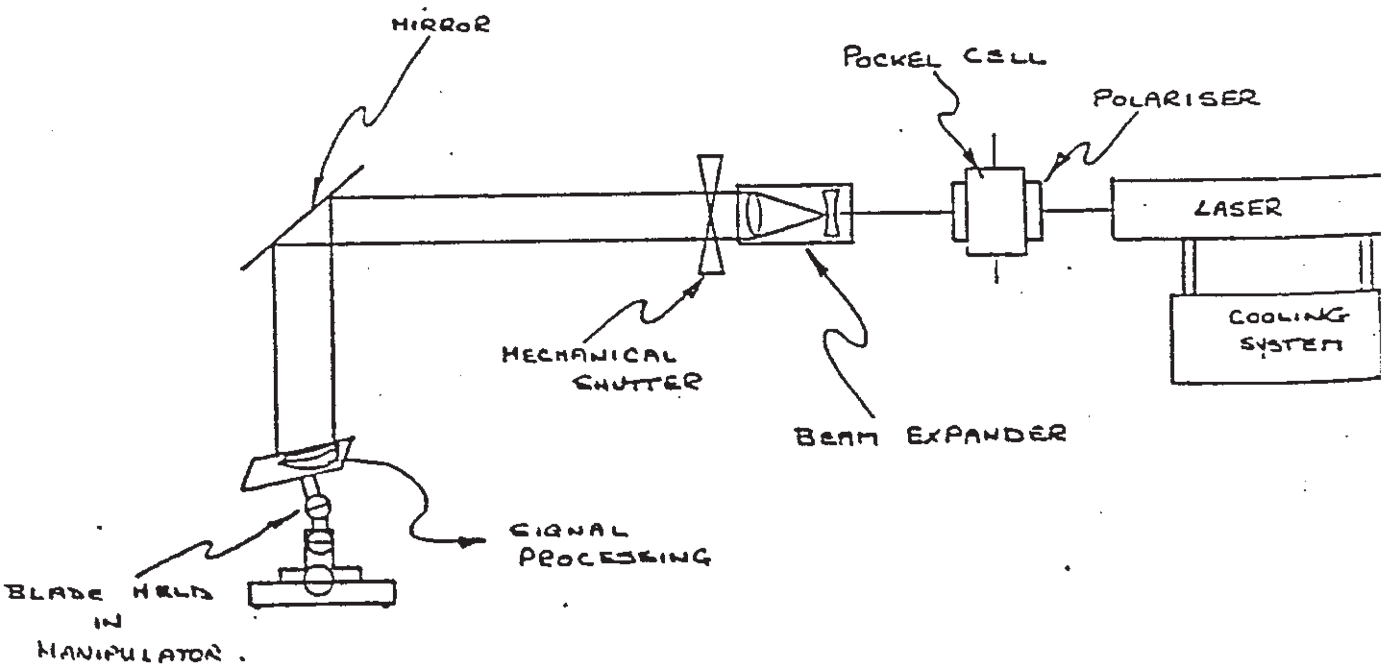

Fig. 13 Laser calibration experimental apparatus.

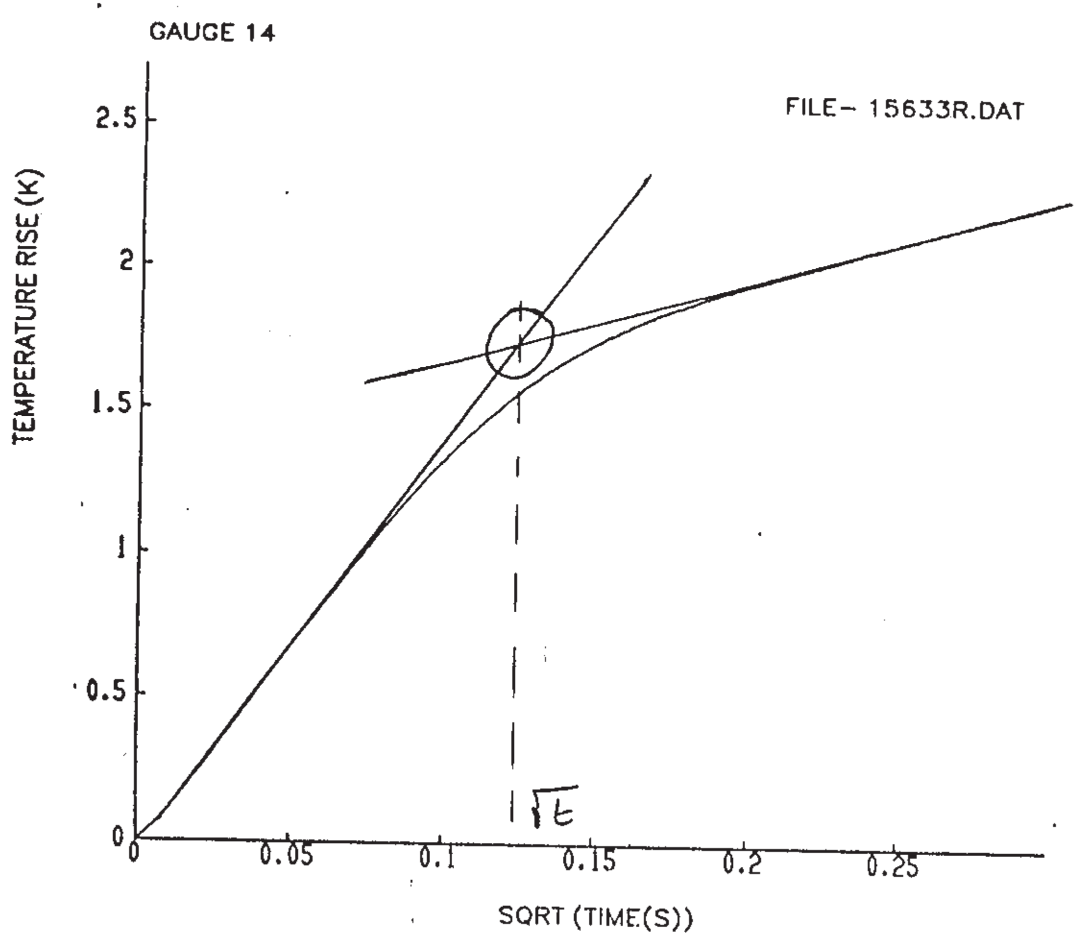

Fig. 14 Typical laser calibration result showing temperature plotted against $\sqrt{\text{time}}$.

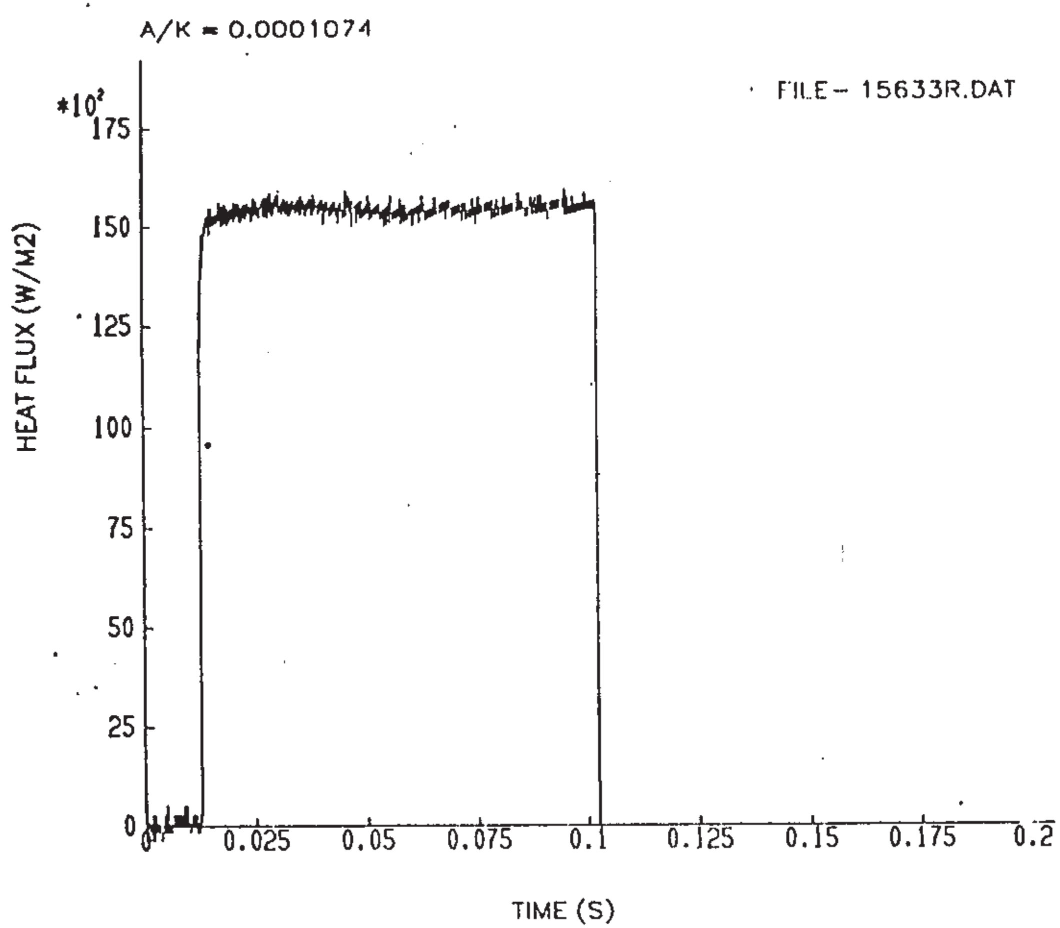

Fig. 15 Reconstructed heat flux input.

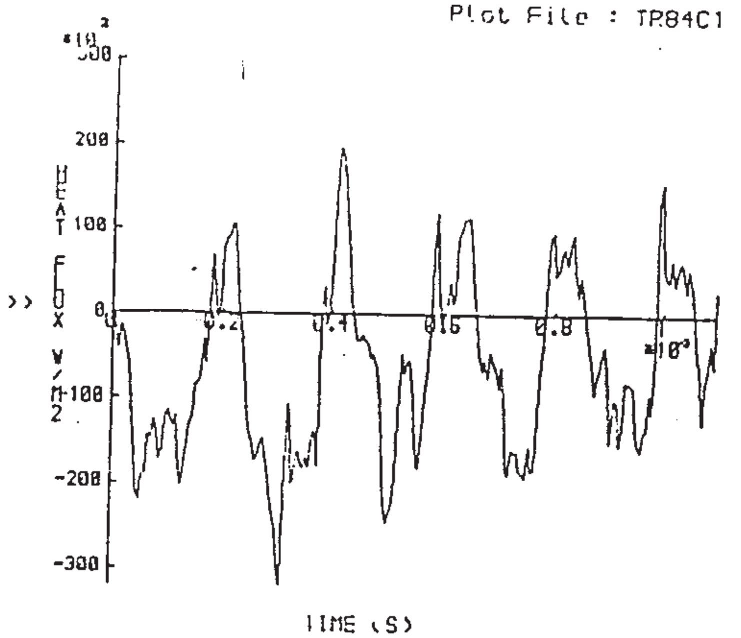

Fig. 16 Typical high frequency heat flux history.

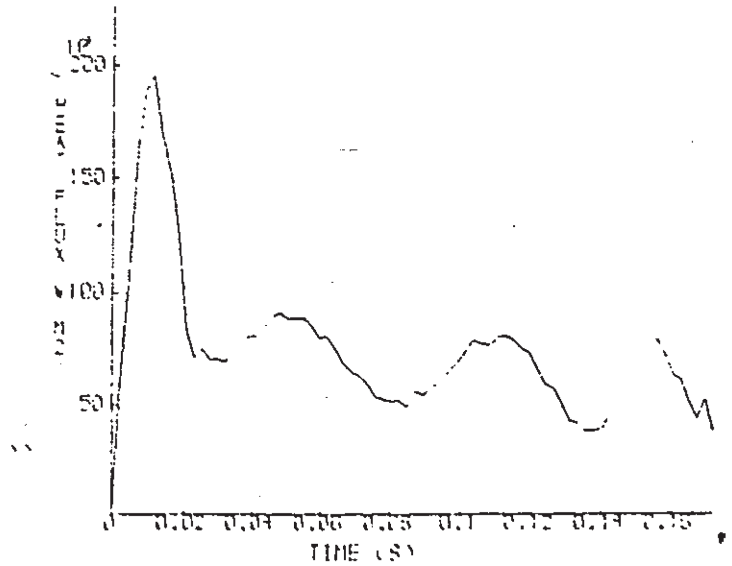

Fig. 17 Typical mean heat flux as function of time.